Asian Journal of Chemistry; Vol. 37, No. 10 (2025), 2561-2570
ASIAN JOURNAL OF CHEMISTRY
https://doi.org/10.14233/ajchem.2025.34438

Photophysical and Spectroscopic Insights into the Interaction Mechanism of Azo-Ester Dye with Ovalbumin: A Molecular Docking Perspective

A. GOPALAKRISHNAN[1], B. SUDHARSAN[1], P. RAJALAKSHMI[1], R. KUMARAN[1], M. VANJINATHAN[1,*] and A. SUBRAMANI[2,*]

[1]PG and Research Department of Chemistry, Dwaraka Doss Goverdhan Doss Vaishnav College, Chennai-600106, India
[2]PG and Research Department of Biochemistry, Dwaraka Doss Goverdhan Doss Vaishnav College, Chennai-600106, India

*Corresponding authors: E mail: mvanjinathan@gmail.com; subramani@dgvaishnavcollege.edu.in

Received: 11 July 2025 *Accepted*: 23 September 2025 *Published online*: 30 September 2025 AJC-22141

In this work, an azo-ester dye with phenol blocked isocyante and *N,N′*-dialkanol groups at the ends were studied as fluorescent probe for protein detection. The photophysical properties of the azo-ester dye were characterized both in its unbound state and in the presence of a globular protein like ovalbumin. Upon increasing concentrations of ovalbumin, a significant enhancement in fluorescence intensity was observed, indicating strong interaction between the dye and the protein. The formation of a 1:1 host-guest complex was further supported by competitive binding experiments using hydrogen-bonding molecules such as urea and guanidine hydrochloride (GuHCl), which disrupted the dye-protein complex and led to the formation of solute-protein hydrogen-bonded interactions instead. Molecular docking studies provided the additional insight into the binding mechanism, revealing a negative docking score for the dye-ovalbumin complex, attributed to hydrogen bonding, π–π stacking and multiple hydrophobic interactions. These findings suggest that the dye binds strongly to ovalbumin and may play a role in modulating its activity, highlighting potential applications in therapeutic strategies and cancer prevention.

Keywords: Ovalbumin, Fluorescent probe, Protein detection, Photophysical properties, Fluorescence, Host-guest complex.

INTRODUCTION

Organic dyes, especially azo compounds, have long been used as traditional photosensitizers in applications such as photodynamic therapy [1,2]. Among these, azo-ester dyes stand out due to their distinctive physico-chemical and photochemical properties as well as their medicinal potential [3,4]. Studying the interactions between dye and proteins is essential in drug design, as it provides valuable insights into pharmacodynamics and pharmacokinetics [5-9]. These interactions typically involve non-covalent forces such as hydrogen bonding, hydrophobic effects and electrostatic interactions that can profoundly affect protein structure and function, particularly when fluorescent probes are employed [10,11].

Ovalbumin (OVA), a 385-residue glycoprotein from egg white with a molecular weight of ~45 kDa, belongs to the serpin superfamily but lacks serine protease inhibitor activity [12-14]. It is widely used in food, pharmaceutical and immunological studies. Structurally, OVA comprise nine α-helices, three β-sheets and three tryptophan residues (Trp148, Trp184, and Trp267), which contribute to its intrinsic fluorescence [13,15]. The protein has an isoelectric point of 4.5 and comes in different phosphorylated forms (A1, A2, and A3) [16]. Though several crystal structures of OVA exist, detailed studies of its interaction with azo-ester dyes remain limited [17,18].

Fluorescence spectroscopy, supported by molecular docking, has proven to be an effective tool for characterizing dye-protein interactions [19-21]. These techniques help determine binding affinities, conformational changes and interaction forces. For example, the quercetin-OVA studies revealed binding constants in the order of 10^4 L mol^{-1}, driven by hydrogen bonding and hydrophobic interactions [21]. Other studies involving bovine serum albumin (BSA) and molecules like atorvastatin and glutathione also demonstrated fluorescence quenching, wavelength shifts, and structural alterations upon binding [10,22].

Numerous investigations have explored OVA interactions with compounds such as curcumin, sulfonamides, resveratrol, aspirin, *etc*. [23-25], consistently highlighting the roles of hydrogen bonding and hydrophobic effects in stabilizing dye-

protein complexes [26-30]. Advanced methods like real-time quartz crystal microbalance and computational docking further enhance the understanding of these interactions [31].

Fluorescence modulation can occur *via* inner filter effects, collisional quenching or structural changes upon ligand binding [32,33]. Molecular docking, a computational technique to predict the ligand-protein binding modes, complements experimental studies by providing insights into binding sites and affinities. A more negative docking score generally indicates stronger binding affinity and this approach has become a cornerstone in drug discovery, significantly reducing time and cost [34-36]. Despite extensive studies on various dye-protein systems, no systematic investigation has been reported on fluorophores bearing azo, ester, phenyl carbamate and *N*,*N*′-dialkanol groups interacting with OVA.

To address this gap, a multifunctional azo-ester dye (Fig. 1) was synthesized and explored its interaction with OVA using UV–visible and fluorescence spectroscopies. The dye was designed with structural features such as azo groups (for *cis*–*trans* isomerization), ester linkages (to enhance flexibility), and phenyl carbamate/*N*,*N*′-dialkanol amines (to mimic peptide bonds and reduce rigidity) making it an ideal candidate for binding to globular proteins like OVA. The role of competitive hydrogen bonding using solutes like urea and guanidine hydrochloride (GuHCl) were also evaluated and performed molecular docking to confirm the binding mechanism and site.

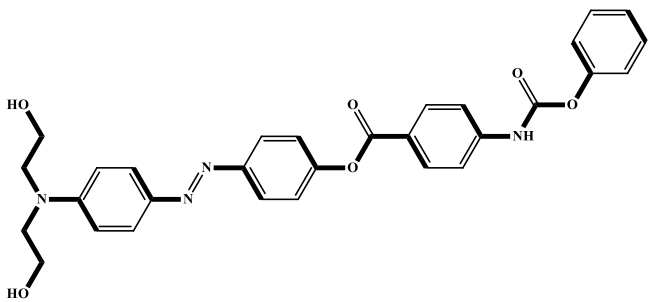

Fig. 1. Structure of azo-ester fluorophore

EXPERIMENTAL

Ovalbumin was procured from Sigma-Aldrich Chemical Co., while urea and guanidine hydrochloride (GuHCl) were obtained from SRL, India). All chemicals were of analytical grade and used without further purification.

Synthesis of azo-ester dye: The azo-dye was synthesized according to the reported procedure [37]. In brief, diazotized 4-aminophenol was reacted with *N*,*N*-*bis*[2-hydroxyethyl]-aniline (**1**) to obtain a red-orange precipitate **2**, which was filtered and washed. In the second step, 4-amino-benzoic acid was acylated with phenyl chloroformate in dry THF to yield 4-{(benzoxycarbonyl)imino}benzoic acid (**3**). This intermediate was then treated with $SOCl_2$ under reflux to convert the carboxylic acid group into the corresponding acid chloride **3**. This acid chloride dissolved in dry THF was added dropwise to a mixture of *N*,*N*′-*bis*(2-hydroxyethyl)-4-(4-hydroxyphenylazo)aniline (**2**), triethylamine and DMAP at 0 ºC under N_2 atmosphere. The product was purified by column chromatography using hexane:ethyl acetate (4:1) (**Scheme-I**).

Preparation of stock solutions of dyes and proteins: Azo-ester dye stock solutions were prepared by dissolving the weighed amount of dye in DMSO to obtain a final concentration of 2 mM. Ovalbumin (OVA) stock solutions were prepared by dissolving the protein in 0.05 M Tris-HCl buffer (pH 7.9) at a concentration of 0.2 mg/mL, corresponding to approximately 4.5 µM.

Preparation of working solutions of dyes and proteins: Working solutions of dye were prepared by dilution of the dye stock solution in 0.05 M Tris-HCl buffer (pH 7.9), 0.05 M phosphate buffer (pH 6.0), 0.05 M Tris-HCl (pH 9.0), in water. Working solutions of the dye in the presence of proteins were prepared by the addition of aliquot of the dye stock solution to the protein stock solution. The concentrations of dye working solutions amounted to 5 µM except for absorption spectra measurements where it was equal to 10 µM. All working solutions were prepared immediately before the experiments

Spectral measurements: Spectroscopic measurements were performed in a standard quartz cuvette (10 × 10 mm). Fluorescence excitation and emission spectra were registered using the fluorescent spectrophotometer Cary Eclipse (Varian, Australia). Absorption spectra were registered using the spectrophotometers Genesys 20 (ThermoScientific) and Shimadzu UV-3600. All the spectral-luminescent characteristics of dyes were studied at room temperature.

Ligand and protein preparation: The 3D structures of synthesized compounds were constructed by maestro builder panel. The ligand preparation wizard was used to add hydrogen atoms and regulate the rational bond angles, geometry and ring conformations. The most favourable ionization states of the compounds were generated using the OPLS-2005 (Optimized Potentials for Liquid Simulations) force field. Geometry optimization was then performed until the structure converged to a root-mean-square deviation (RMSD) cutoff of 0.01 Å, ensuring a minimized energy conformation [38]. The subsequent output structure of compounds was suitable for docking with protein Ova.

The crystal structure of the ovalbumin (PDB-1OVA) was downloaded from the protein data bank (http://www.rcsb.org). The receptor was fully optimized in the protein preparation wizard, which involved adding polar hydrogen atoms, assigning bond orders, determining protonation states and subsequently removing water molecules beyond a 5 Å distance. Thereafter, by using force field (OPLS-2005) the energy minimization of 0.03 Å RMSD was performed to reduce the steric hindrance caused by the addition of hydrogen atoms. Now the minimized OVA receptor was suitable for docking by supplied x, y and z coordinates 45.14, -7.99 and -8.72 Å, respectively with grid box diameter (xyz) of 30 × 30 × 30 Å. The chemical structures from Chem-Draw were transformed into energy-optimized PDB (Protein Data Bank) format using Chem 3D 17.0. This conversion allows the representation of the compounds in a suitable format for further computational analysis and modelling. Pymol software was used for the visualization of the docked molecules.

RESULTS AND DISCUSSION

Absorption and emission studies of dye: The absorption spectrum of azo-ester dye at 10^{-6} M in water exhibit peaks

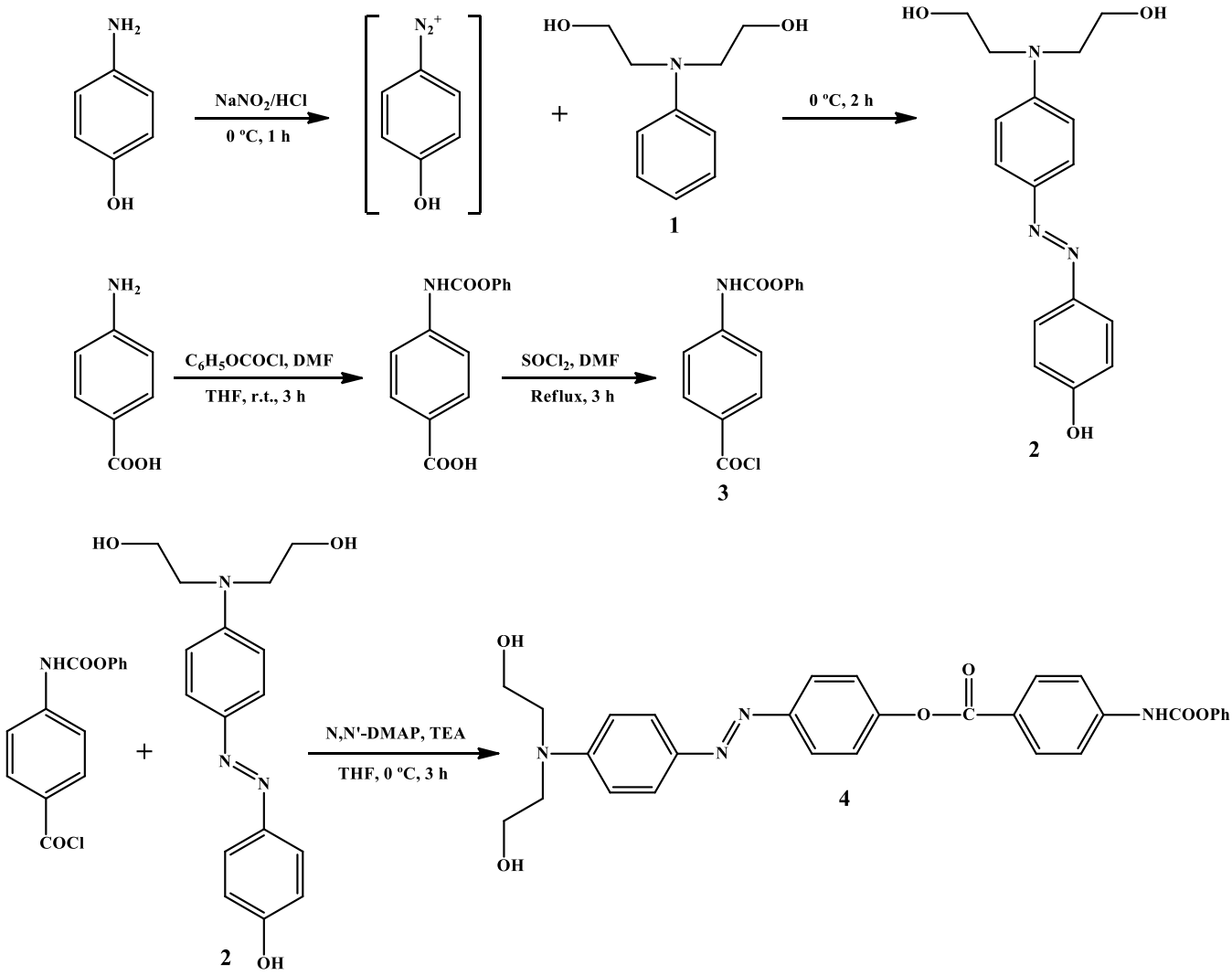

Scheme-I: Synthetic route of azo-ester dye [Ref. 39]

at 290 and 450 nm (Fig. 2a). The π-π* transition is due to the absorption peak at 290 nm indicating that there will be conjugation in the dye whereas the n-π* transition is responsible for the peak at 450 nm, which indicates the presence of heteroatom in the synthesized fluorophore. When electron-donor and electron-acceptor groups are positioned at the 4- and 4′-positions of azobenzene chromophore, the dipole moment of the molecule increases. This effect leads to an increment in the charge transfer (CT) character of the π-π* transition across the long axis of the molecule. Thus, an enhancement of the CT character gives rise to a red shift of the π-π* transition band, which then overlaps the weak n-π* transition band. Moreover, the polarity of the solvent has a strong influence on the position of this band due to its CT character [39]. The synthesized azo ester dye is organic nature and found to be insoluble in solvent like water, but it is worth to mention that its solubility in water is very low and we carried out all the experiments in this work as a concentration of 10^{-6} M in H_2O.

The emission spectra of dye at 10^{-6} M concentration are shown in Fig. 2b. The absorption peaks observed at 290 nm and 450 nm on excitation give emission at 326 nm with an intensity of 900 while there is no emissive peak observed at 450 nm. This behaviour can be attributed either to non-radiative transitions or to high-energy electronic transitions whose corresponding wavelengths fall in the far-UV region, outside the typical spectroscopic range of 200-800 nm. Moreover, the dye in a polar solvent such as water exhibits a Stokes shift of 36 nm. This shift is significantly influenced by solvent polarity; in polar environments, stabilization of the excited state relative to the ground state leads to an increased Stokes shift. Thus, the presence of polar solvents causes a significant red shift in the fluorescence emission.

Absorption and emission studies of ovalbumin (OVA): The UV-vis spectrum of OVA at 10^{-6} M concentration (Fig. 3a) exhibits an absorption peak at 290 nm with an absorbance of 0.41, which is due to almost entirely π-π* transitions in the peptide backbone of the proteins. Absorption in the range of 230-300 nm is dominated by the aromatic side-chains of tryptophan (Trp), tyrosine (Tyr) and phenylalanine (Phe) residues and there is a weak contribution by disulfide bonds near 260 nm in the absorption spectrum.

In OVA, the residues TRP148, TRP184 and TRP267 act as the principal intrinsic fluorophores and play a key role in the structural changes during ligand binding [40]. Therefore, to

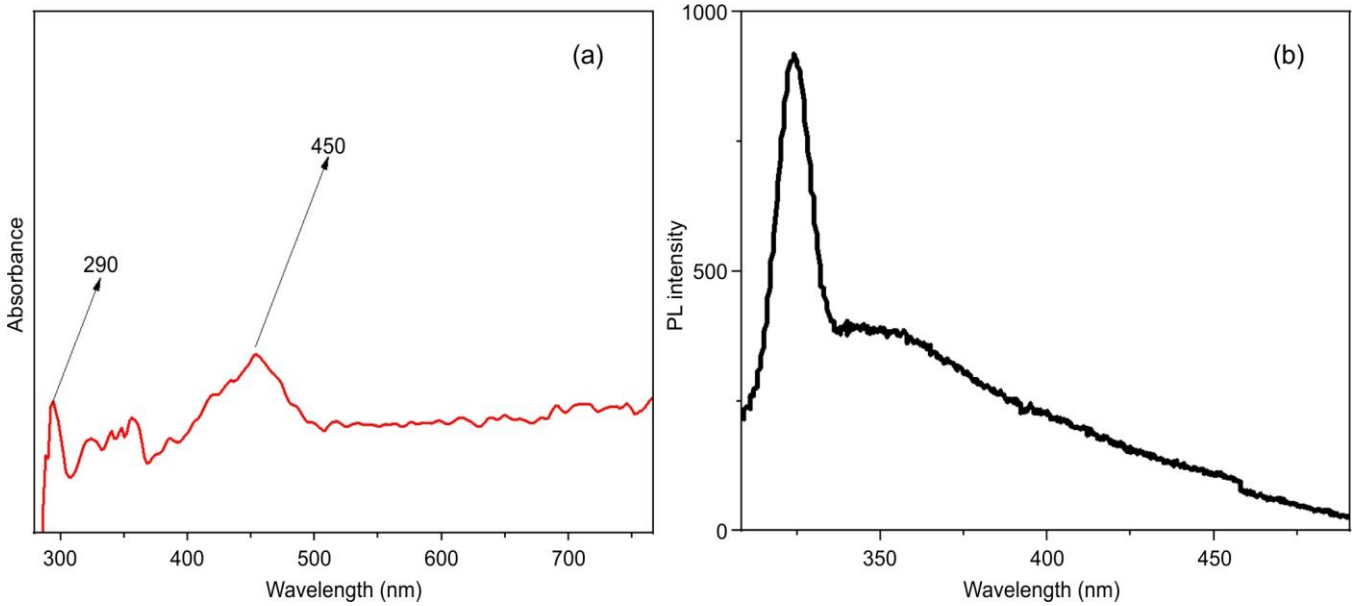

Fig. 2. (a) UV-vis spectrum of dye measured at concentration of 10^{-6} M in H_2O, (b) emission spectrum of dye measured at a concentration of 10^{-6} M in H_2O on excitation at 290 nm

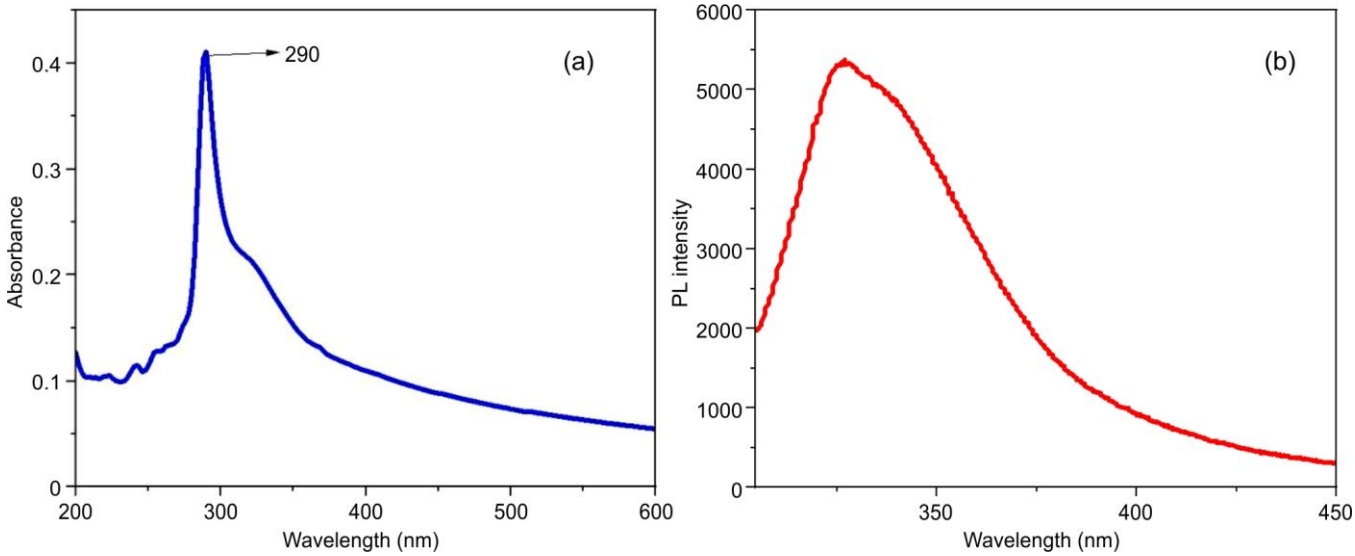

Fig. 3. (a) UV-vis spectrum of ovalbumin measured at a concentration of 10^{-6} M in H_2O, (b) emission spectrum of ovalbumin measured at a concentration of 10^{-6} M in H_2O on excitation at 290 nm

investigate the conformational dynamics and ligand interactions, the fluorescence emission spectra of native OVA were analyzed. Changes in emission can reveal alterations in the tertiary structure, highlighting the role of specific Trp residues as sensitive reporters of protein-ligand interactions. Amino acid residues, such as tryptophan residues (TRP148, TRP184 and TRP267) are the major fluorophores.

Fig. 3b displays the emission spectrum of OVA measured at 10^{-6} M in H_2O on excitation at 290 nm, the maximum emission wavelength for the OVA was observed at 343 nm. This can be attributed to the presence of tryptophan residue present in the OVA. The tryptophan emission analysis helps to reveal the information about the conformational changes of OVA protein and avoids the contribution of tyrosine residue [41]. This was accomplished by selecting 295 nm as the excitation wavelength for the OVA protein.

UV-Visible absorption spectral studies of OVA with varying azo-ester dye concentration: According to Tian *et al.* [42] when the protein-ligand interaction mechanism occurs by dynamic quenching, the UV-vis absorption spectrum of the protein is not altered in the presence of the ligand, as this is caused by collisions between the fluorophore in the excited state in the protein and the ligand. In our present study, upon addition of various concentrations of azo-ester dye (10^{-6} to 10^{-8} M) to fixed concentration of OVA (10^{-6} M) does not cause any change in the UV-visible absorption spectra (spectra not shown).

UV-Visible spectral studies of azo-ester dye with various concentrations of OVA: To determine the ideal conditions for the interaction to occur, the UV-vis absorption spectra of OVA at different concentrations (10^{-6} M to 10^{-8} M) with a fixed dye concentration (10^{-6} M) were examined. The

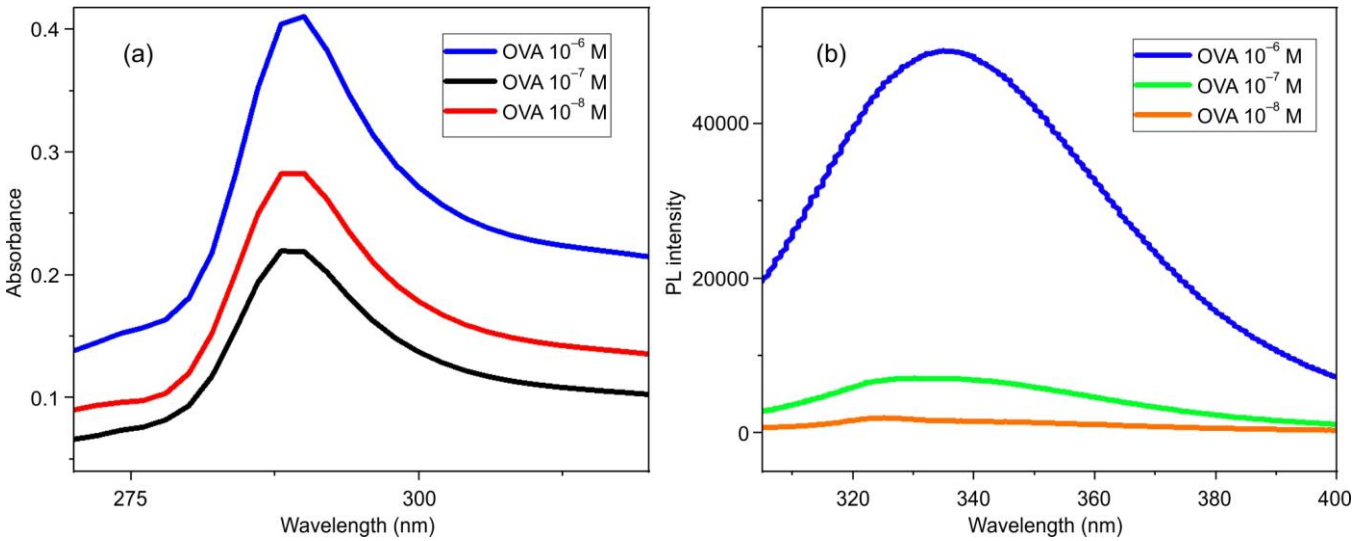

Fig. 4. (a) UV-vis spectrum of various concentrations of ovalbumin with dye 10^{-6} M, (b) emission spectra of various concentrations of ovalbumin on excitation at 290 nm

UV spectra of different concentrations in water such as 10^{-6} M, 10^{-7} M and 10^{-8} M, reveal that all concentrations have an absorption peak at 290 nm, with absorption values of 0.41, 0.28 and 0.21, respectively (Fig. 4a). Upon titration with increasing concentrations of OVA, the absorption intensity of the azo-ester dye gradually increased, accompanied by a notable red shift of approximately 6 nm. This shift indicates an increase in the hydrophobicity of the microenvironment surrounding the aromatic amino acid residues of OVA, suggesting the conformational change upon binding. The observed spectral changes may also be attributed to alterations in the oscillator strength of the dye's chromophore. These findings support the formation of a specific, non-electrostatic interaction between the azo-ester dye and OVA [43]. Furthermore, the spectral behaviour is consistent with the formation of a 1:1 stable dye-protein complex.

Emission spectral studies of azo-ester dye with various concentrations of OVA: Tryptophan residues (TRP148, TRP184 and TRP267) are the major fluorophores in OVA and play a crucial role in conformational (quaternary structure) changes upon drug interaction. To monitor these conformational changes, tryptophan fluorescence emission was analyzed, using an excitation wavelength of 295 nm. This wavelength selectively excites tryptophan while minimizing interference from tyrosine residues [44]. The emission spectra of OVA at different concentrations, *e.g.* 10^{-6} M, 10^{-7} M and 10^{-8} M are shown in Fig. 4b. Upon excitation at 290 nm, emission peaks were observed at 326 nm for all concentrations, with fluorescence intensities of 49000, 6800 and 1900, respectively. These results indicate a concentration-dependent increase in fluorescence intensity. The enhancement in fluorescence suggests a strong interaction between OVA and the azo-ester dye, likely involving hydrophobic amino acid residues. This interaction appears to expose previously buried tryptophan residues to a more hydrophilic environment, which aligns with previously reported studies [45].

The presence of dye molecules in structures such as hydrogen-bonded self-assemblies, inclusion complexes or micelles is known to enhance protein fluorescence, suggesting that the dye may bind within the hydrophobic cavities of the protein [46]. Significantly, the 1:1 OVA:dye molar ratio (10^{-6} M each) resulted in the highest fluorescence intensity (49000), indicating the formation of a stable 1:1 complex.

Encouraged by the absorption and fluorescence findings, further studies were conducted to understand the interaction mechanism between OVA and the dye. Absorption measurements showed a gradual increase in absorbance with protein concentrations from 10^{-8} M to 10^{-7} M, followed by a sharp increase from 10^{-7} M to 10^{-6} M (Fig. 5), further supporting complex formation. To probe the nature of the interactions, additional experiments were conducted using hydrogen bonding disruptors such as urea and guanidine hydrochloride (GuHCl). The observed linear relationship in these studies supports the formation of a 1:1 stoichiometric complex between OVA and the azo-ester dye, likely stabilized by hydrophobic and hydrogen bonding interactions.

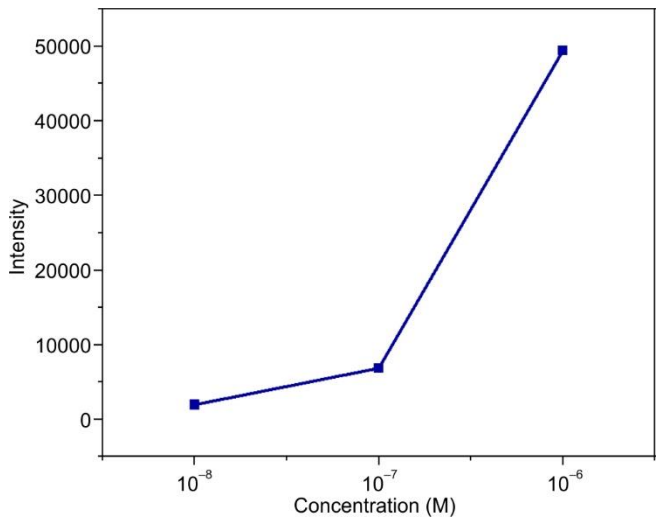

Fig. 5. Variation of OVA concentration with respect to absorption intensity

Effect of hydrogen bonding solutes on OVA-azo-ester dye complex: Both urea and GuHCl have strong hydrogen-

bonding capabilities with solvents and can change the structure of water. Research on GuHCl [47] primarily focusses on the ideas of protein folding and refolding, RNA isolation and inhibition, hydrophobic interaction disruption and the solubility of hydrophobic amino acids in water. In comparison to urea in aqueous solutions, the inclusion of an imine and aminoacetal moieties in GuHCl results in a larger change in the H-bonding characteristics (number of H bonding acceptor and donor groups). The photophysical properties of an extrinsic fluorescent probe with GuHCl is less compared to that of urea interaction with fluorescent probes in water, and the change in the photophysical properties of probes with high chemosensitive compounds like GuHCl is an uncharted area [48].

UV-visible and fluorescence spectral studies of interaction of urea with 1:1 OVA and azo-ester dye complex: The UV-visible spectra of different concentrations of urea are depicted in Fig. 6. The (dye + OVA) mixture with a 1:1 ratio (10^{-6} M) reveals no notable change in the wavelength of 290 nm for all the mixtures and the absorption value of a 1:1 mixture is 0.32 while adding hydrogen bonding solutes like 0.1 M of urea to the 10^{-6} M of dye and protein, there is a decrease in the absorption intensity from 0.32 to 0.09 this shows that there involves a weak interaction between dye and protein. This is most likely due to the interaction in ground state, which further decrease in the concentration of urea from 0.1 M to 10^{-5} M, there will be a further decrease in the absorption intensity from 0.06 there will be a three-fold decrease between the different concentrations of urea. This is probably due to the formation of a relatively stable adduct between the urea and OVA-dye complex, in comparison to the already existing urea-dye and urea-protein complex.

The fluorescence spectra of various concentrations of urea to the 1:1 mixture of dye-OVA is shown in Fig. 7. The addition of 10^{-5} M urea to the 1:1 mixture of OVA-dye on excitation at 290 nm gives an emissive peak at 326 nm with an intensity of 4500 while the intensity of 1:1 ratio was 49000 and also there involves the appearance of two new peaks at 363 and 430 nm on excitation at 320 nm and 370 nm, respecttively, with intensities of 660 and 190, respectively. It should be mentioned that these two new emission peaks observed at 363 and 430 nm were not observed in the any of the dye-protein complex and also where the peaks was not observed in a 1:1 ratio of OVA-dye complex. This indicates that there is a formation of a new urea-OVA complex rather than an dye-OVA complex.

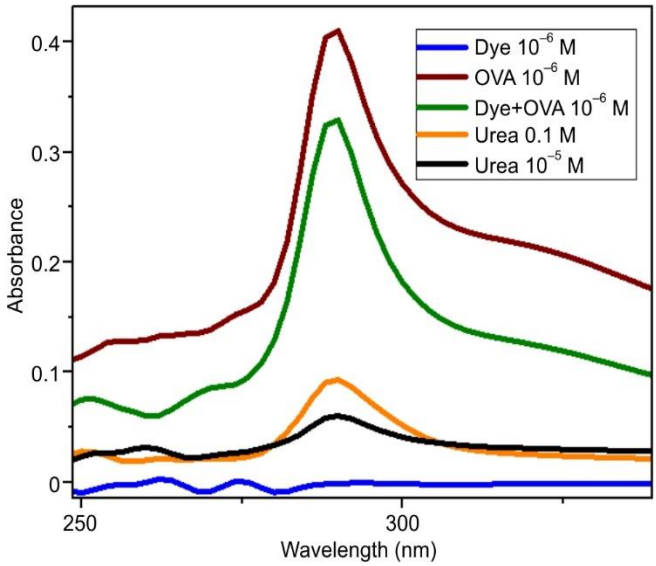

Fig. 6. UV-vis spectra of a mixture of dye + OVA (1:1) in various concentrations of urea

The fluorescence spectra of different concentrations of urea to the 1:1 mixture of dye-OVA is shown in Fig. 7. The addition of 10^{-5} M urea to the 1:1 mixture of dye-OVA on excitation at 290 nm gives an emissive peak at 326 nm with an intensity of 4500 while the intensity of the 1:1 ratio was 49000 and also there involves the presence of two new peaks at 363 and 430 nm on excitation at 320 nm and 370 nm, respectively, with intensities of 660 and 190 respectively. Here it should be mentioned that these two new emission peaks observed at 363 and 430 nm were not noted in the any of the dye-OVA complex and also where the peaks was not observed in a 1:1 ratio of OVA-dye complex. This indicates that there is a formation of a new urea-Ova complex rather than an OVA-dye complex

Further, increase in concentration of urea from 10^{-5} M to 10^{-1} M the intensity of emission on excitation of 290 nm gives 4800 at 326 nm while the other two peaks (363 and 430) give intensities at 920 and 350, respectively which is approximately three-folds and two-fold increments when compared to 10^{-5} M urea. An increase in concentration results in higher

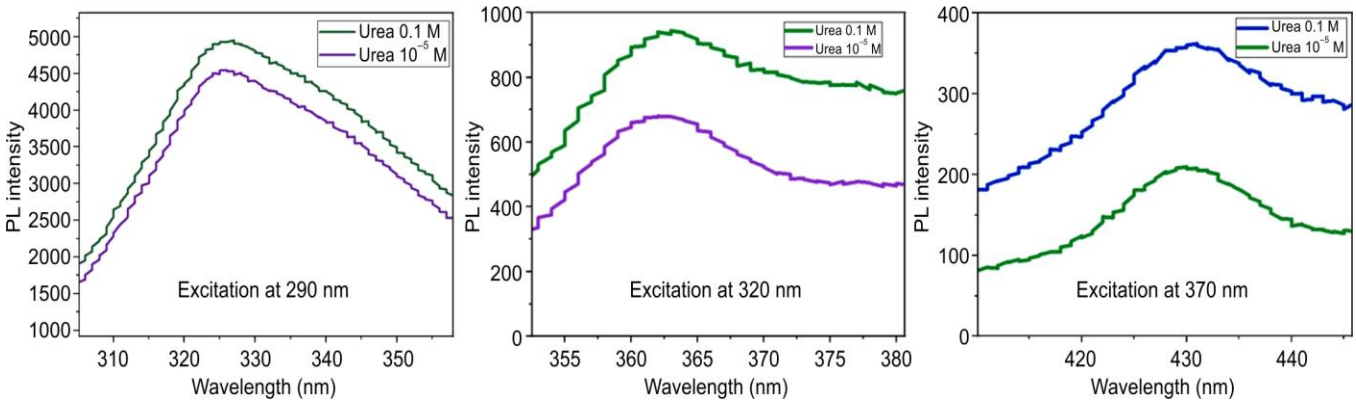

Fig. 7. Emission spectra of a mixture of dye with ovalbumin of 1:1 ratio (10^{-6} M) of various emission wavelengths of 0.1 M and 10^{-5} M concentrations of urea

emission intensities, suggesting the involvement of both ground and excited state interactions. This enhancement indicates the formation of a more stable and stronger OVA-urea complex. The interaction leads to the formation of a new host-competitive guest complex, causing the breakdown of the OVA-dye host-guest complex. In the 1:1 OVA-dye complex, the trypotphan residues are buried within the protein structure. However, the addition of hydrogen-bonding solutes like urea increases the intensity and generates new peaks at 320 nm and 370 nm. These new peaks correspond to the previously buried trypotphan residues being exposed on the surface, confirming their relocation through this spectral shift [49].

UV-visible and fluorescence spectral studies of interaction of GuHCl with 1:1 OVA and azo-ester dye complex: To further investigate the hydrogen bonding effects, GuHCl was used as a competing solute. As shown in Fig. 8, the 1:1 mixture of azo-ester dye and OVA at a concentration of 10^{-6} M exhibits an absorption maximum at 290 nm, with an intensity of 0.32. Upon the addition of 0.1 M GuHCl, a significant decrease in absorption intensity from 0.32 to 0.08 was observed, suggesting a weakening of the dye–protein interaction, likely due to ground-state complex disruption. A further reduction in GuHCl concentration from 0.1 M to 10^{-5} M resulted in an additional decrease in absorption to 0.06, indicating a concentration-dependent competitive interaction, where GuHCl increasingly dominates the binding site.

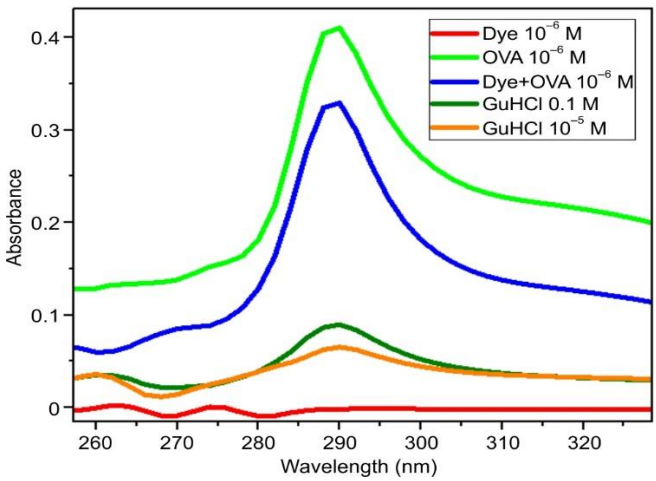

Fig. 8. UV-vis spectra of mixtures of dye + Ova (1:1) in various concentrations of guanidine hydrochloride

Fig. 9 displays the emission spectra of the dye–OVA complex upon titration with GuHCl. The addition of 10^{-5} M GuHCl to the 1:1 dye–OVA mixture, excited at 290 nm, results in an emission peak at 326 nm with an intensity of 4700, compared to 4900 for the unmodified 1:1 complex. Additionally, two new emission peaks emerge at 363 nm and 430 nm, upon excitation at 320 nm and 370 nm, with intensities of 750 and 280, respectively peaks absent in the dye–OVA complex alone. These spectral changes strongly indicate the formation of a new OVA–GuHCl complex, displacing the original dye from its binding site.

As the GuHCl concentration increases from 10^{-5} M to 10^{-1} M, the emission intensity at 326 nm further increases to 5000, and the corresponding intensities at 363 nm and 430 nm rise to 840 and 310, respectively. This trend confirms that increasing GuHCl concentration enhances emission intensity, supporting the involvement of both ground- and excited-state interactions. The observed spectral shifts and new peaks suggest a competitive host–guest interaction, wherein GuHCl replaces the dye, forming a more stable OVA–GuHCl complex. This complex formation likely exposes previously buried tryptophan residues, as indicated by the appearance of new emission peaks associated with their transition to a more solvent-accessible environment.

Docking studies of OVA-azo-ester dye complex: Molecular docking study was performed to determine the basic binding location of OVA to azo-ester dye [50]. The finest interaction position of organic compounds with select protein is visualized in Fig. 10 and data are summarized in Table-1. The observed docking score value of azo-ester dye is -5.753 kcal/mol. The docking score results revealed that dye molecules are well located in the hydrophobic site and strongly associate with the ovalbumin receptor *via* π-π stacking, hydrophobic, and H-bonding connections. The dye displayed the negative docking score, which was controlled by hydrogen bond with residue ASN B:49, ASN D:91, PRO B:391, GLU A:339 and π-π stacking ARG B:170, LYS A:292 numerous hydrophobic contacts like VAL D:90, ILE B:168, MET A:291, MET B:293, PRO B:391. Based on the information above, the dye binds and organizes the ovalbumin function in a way that promotes the healing and prevents cancer.

Frontier molecular orbital (FMO) analysis: The calculated HOMO and LUMO energy levels offer critical insight into the electronic, chemical and optical properties of the mole-

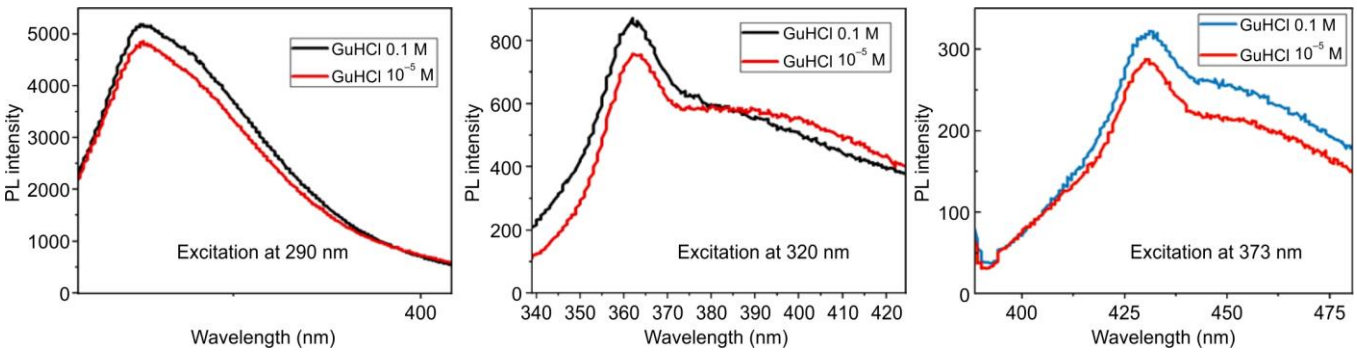

Fig. 9. Emission spectra of mixtures of dye with ovalbumin of 1:1 ratio (10^{-6} M) of various emission wavelengths of 0.1 M and 10^{-5} M concentrations of guanidine hydrochloride

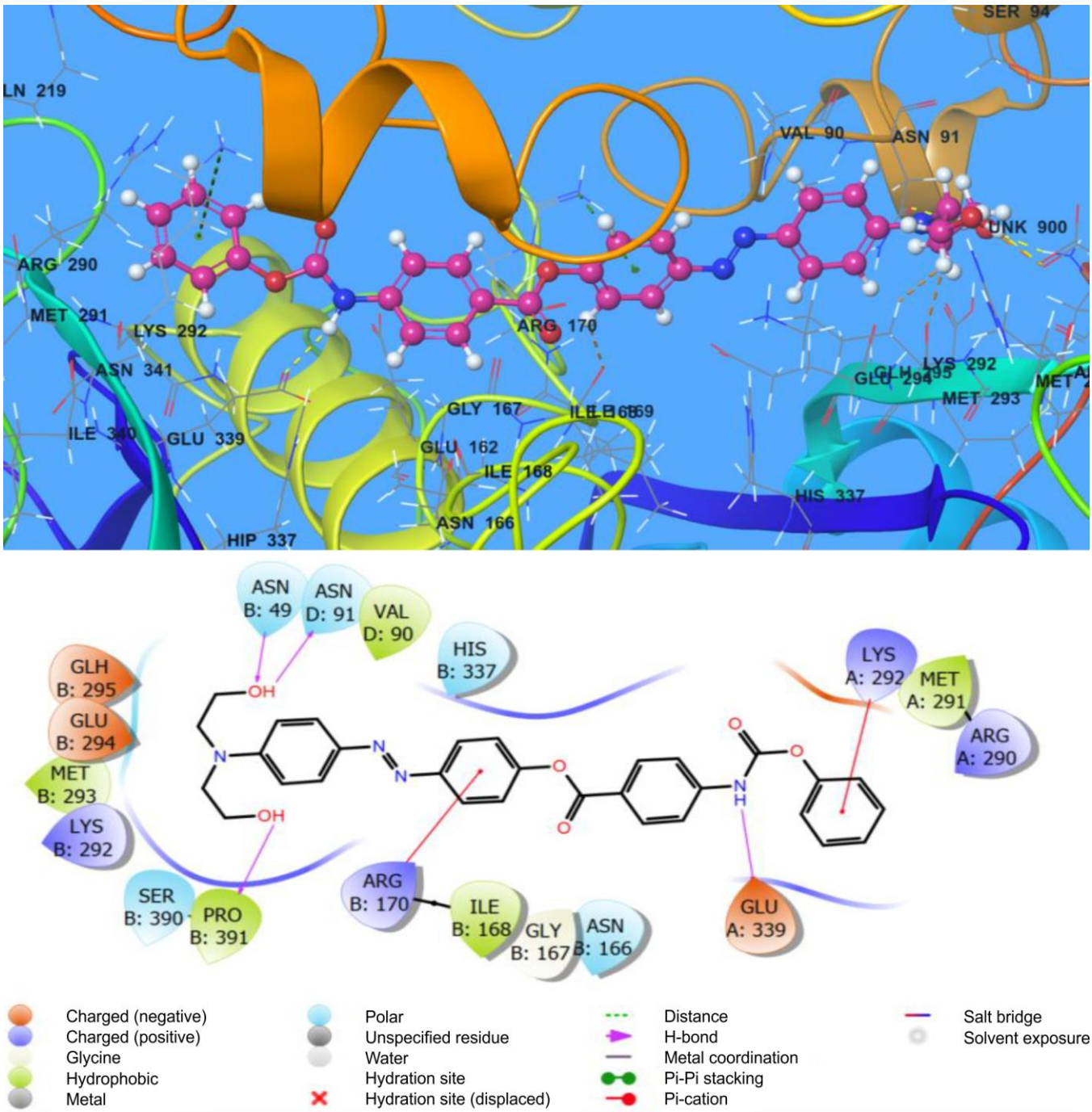

Fig. 10. 3D and 2D interactions of the compound **1** with the receptor ovalbumin

TABLE-1
MOLECULAR DOCKING PARAMETERS OF THE SYNTHESIZED COMPOUNDS WITH OVALBUMIN RECEPTOR

Compound	Docking score (kcal mol^{-1})	Active sites with a mode of interaction		
		H-bond	π-π stacking	Hydrophobic contacts (cut-off at 5 Å)
Azo-ester dye	-5.753	ASN B:49, ASN D:91, PRO B:391, GLU A:339	ARG B:170, LYS A:292	VAL D:90, ILE B:168, MET A:291, MET B:293, PRO B:391

cule [30]. The LUMO, in particular, plays a key role in dictating chemical reactivity as well as the electronic and optoelectronic behaviour of molecule. The HOMO–LUMO energy gap (ΔE) is an important parameter to assess molecular stability, reactivity and polarizability.

In this study, the quantum chemical calculations revealed E_{HOMO} = –5.107 eV and E_{LUMO} = –2.014 eV, resulting in a ΔE of 3.093 eV. A lower ΔE value indicates higher reactivity, greater polarizability and lower kinetic stability, characteristics typically associated with the soft molecules. The negative

energy values reflect the convention where zero energy corresponds to an electron at infinite separation from the molecule; thus, any bound electron (in HOMO or LUMO) exists in a more stable, negative energy state. The relatively low band gap of the synthesized dye suggests facilitated electronic transitions from ground to excited states, which may enhance its photophysical behaviour. Furthermore, this narrow gap is also indicative of potential biological activity, as molecules with smaller ΔE are often more interactive with biological targets.

Conclusion

In this work, the absorption and emission studies had been measured for the ovalbumin-dye fluorophore complex. The addition of ovalbumin results in an increase in the absorbance of the dye. This is attributed to the strong absorbance of ovalbumin, moreover, the variation of concentration of ovalbumin employed influences the absorbance peaks in the visible region significantly compared to the UV region. The formation of the host-guest complex is confirmed by the addition of competing guest molecules like urea and guanidine hydrochloride to the OVA-dye complex, which resulted in the breakdown of the host-guest complex. Fluorescence studies of dye-OVA resulted in a broad emission peak and intensity values showing the stronger binding complex between dye and OVA. In the presence of hydrogen bonding solutes, the host-competing guest complex was formed. This is further proved by molecular docking studies which show a binding score of -5.753 kcal mol^{-1}. Molecular docking studies were performed to locate the binding site of azo-ester dye in OVA and the interactions with the following residues were confirmed within the binding pocket: ASN B:49, ASN D:91, PRO B:391, GLU A:339, ARG B:170, LYS A:292 VAL D:90, ILE B:168, MET A:291, MET B:293, PRO B:391. The moderate affinity of azo-ester dye for OVA was determined, which is a crucial characteristic for efficient drug binding and release.

CONFLICT OF INTEREST

The authors declare that there is no conflict of interests regarding the publication of this article.

REFERENCES

1. V. Juvekar, C.S. Lim, D.J. Lee, S.J. Park, G.O. Song, H. Kang and H.M. Kim, *Chem. Sci.*, **12**, 427 (2021); https://doi.org/10.1039/D0SC05686C
2. S. Sari, S. Ünver, T. Avsar, Ş. Özçelik, T. Kilic and M.U. Kahveci, *Polym. Chem.*, **15**, 2177 (2024); https://doi.org/10.1039/D4PY00318G
3. Y. Ali, S.A. Hamid and U. Rashid, *Mini-Rev. Med. Chem.*, **18**, 1548 (2018); https://doi.org/10.2174/1389557518666180524113111
4. M.N. Khan, D.K. Parmar and D. Das, *Mini-Rev. Med. Chem.*, **21**, 1071 (2021); https://doi.org/10.2174/1389557520999201123210025
5. M.V. Khan, M. Ishtikhar, G. Rabbani, M. Zaman, A.S. Abdelhameed and R.H. Khan, *Int. J. Biol. Macromol.*, **94**, 290 (2017); https://doi.org/10.1016/j.ijbiomac.2016.10.023
6. G. Rabbani, M.J. Khan, A. Ahmad, M.Y. Maskat and R.H. Khan, *Colloids Surf. B Biointerfaces*, **123**, 96 (2014); https://doi.org/10.1016/j.colsurfb.2014.08.035
7. P. Manivel, S. Anandakumar and M. Ilanchelian, *Luminescence*, **30**, 729 (2015); https://doi.org/10.1002/bio.2812
8. P. Manivel, M. Paulpandi, K. Murugan, G. Benelli and M. Ilanchelian, *J. Biomol. Struct. Dyn.*, **35**, 3012 (2017); https://doi.org/10.1080/07391102.2016.1235513
9. A. Sumita, G. Shoba, R. Thamarai Selvan, K. Anju, M.D. Balakumaran and R. Kumaran, *Results Chem.*, **3**, 100187 (2021); https://doi.org/10.1016/j.rechem.2021.100187
10. A. Jahanban-Esfahlan and V. Panahi-Azar, *Food Chem.*, **202**, 426 (2016); https://doi.org/10.1016/j.foodchem.2016.02.026
11. R.T. Selvan, G. Shoba, M.S. Sangeetha, V.S. Merin, R. Kumaran, P. Tamizhdurai, M. Alanazi and P.S. Ganesh, *J. Saudi Chem. Soc.*, **25** 101364 (2021); https://doi.org/10.1016/j.jscs.2021.101364
12. R. Wang, Y. Yin, H. Li, Y. Wang, J.-J. Pu, R. Wang, H. Dou, C. Song and R. Wang, *Mol. Biol. Rep.*, **40**, 3409 (2013); https://doi.org/10.1007/s11033-012-2418-x
13. R. Rajamanikandan, A.S. Sharma and M. Ilanchelian, *J. Biomol. Struct. Dyn.*, **37**, 4292 (2019); https://doi.org/10.1080/07391102.2018.1550441
14. A.C.F. de Lyra, A.L. dos Santos Silva, E.C.L. dos Santos, A.M.Q. López, J.C.S. da Silva, I.M. Figueiredo and J.C.C. Santos, *Spectrochim. Acta A Mol. Biomol. Spectrosc.*, **228**, 117747 (2020); https://doi.org/10.1016/j.saa.2019.117747
15. J.A. Huntington and P.E. Stein, *J. Chromatogr., Biomed. Appl.*, **756**, 189 (2001); https://doi.org/10.1016/S0378-4347(01)00108-6
16. T. Strixner and U. Kulozik, eds.: G.O. Phillips and P.A. Williams, Egg Proteins, In: Handbook of Food Proteins, Cambridge, UK: Woodhead Publishing, edn 1, pp. 150–209 (2011).
17. E. Remold-O'Donnell, *FEBS Lett.*, **315**, 105 (1993); https://doi.org/10.1016/0014-5793(93)81143-N
18. M.D.D.A. Dantas, H.D.A. Tenorio, T.I.B. Lopes, H.J.V. Pereira, A.J. Marsaioli, I.M. Figueiredo and J.C.C. Santos, *Int. J. Biol. Macromol.*, **102**, 505 (2017); https://doi.org/10.1016/j.ijbiomac.2017.04.052
19. P. Manivel, M. Parthiban and M. Ilanchelian, *J. Biomol. Struct. Dyn.*, **38**, 1838 (2019); https://doi.org/10.1080/07391102.2019.1618734
20. R. Kumaran and P. Ramamurthy, *J. Phys. Chem. B*, **110**, 23783 (2006); https://doi.org/10.1021/jp0628378
21. Y. Lu, Y.-L. Wang, S.-H. Gao, G.-K. Wang, C.-L. Yan and D.-J. Chen, *J. Lumin.*, **129**, 1048 (2009); https://doi.org/10.1016/j.jlumin.2009.04.030
22. Q. Wang, C. Huang, M. Jiang, Y. Zhu, J. Wang, J. Chen and J. Shi, *Spectrochim. Acta A Mol. Biomol. Spectrosc.*, **156**, 155 (2016); https://doi.org/10.1016/j.saa.2015.12.003
23. S. Widyarti, S. Permana, and S.B. Sumitro, *AIP Conf. Proc.* **2021**, 070015 (2018); https://doi.org/10.1063/1.5062813
24. Q. Huang, F. Geng, M. Ma, Y. Jin, J. Fang and S. Sun, *Asian J. Chem.*, **25**, 3692 (2013); https://doi.org/10.14233/ajchem.2013.13724
25. G.E. Jayanti, S. Widyarti, A. Sabarudin and S.B. Sumitro, *Asian J. Pharm. Clin. Res.*, **11**, 340 (2018); https://doi.org/10.22159/ajpcr.2018.v11i7.25440
26. Y. Liu, Y. Cai, D. Ying, Y. Fu, Y. Xiong and X. Le, *Int. J. Biol. Macromol.*, **116**, 893 (2018); https://doi.org/10.1016/j.ijbiomac.2018.05.089
27. M.D.A. Dantas, H.A. Tenório, T.I.B. Lopes, H.J.V. Pereira, A.J. Marsaioli, I.M. Figueiredo and J.C.C. Santos, *Int. J. Biol. Macromol.*, **102**, 505 (2017); https://doi.org/10.1016/j.ijbiomac.2017.04.052
28. X. Fu, T. Belwal, Y. He, Y. Xu, L. Li and Z. Luo, *Food Chem.*, **320**, 126616 (2020); https://doi.org/10.1016/j.foodchem.2020.126616
29. J. Wang, Y. Dadmohammadi, A. Jaiswal and A. Abbaspourrad, *J. Agric. Food Chem.*, **68**, 10184 (2020); https://doi.org/10.1021/acs.jafc.0c03201
30. O.E. Sponton, A.A. Perez, C.R. Carrara and L.G. Santiago, *Colloids Surf. B Biointerfaces*, **128**, 219 (2015); https://doi.org/10.1016/j.colsurfb.2015.01.037
31. J. Wang, Y. Dadmohammadi, A. Jaiswal and A. Abbaspourrad, *J. Agric. Food Chem.*, **68**, 10184 (2020); https://doi.org/10.1021/acs.jafc.0c03201
32. M. van de Weert and L. Stella, *J. Mol. Struct.*, **998**, 144 (2011);

https://doi.org/10.1016/j.molstruc.2011.05.023
33. K.N. Houk, A.G. Leach, S.P. Kim and X. Zhang, *Angew. Chem. Int. Ed.*, **42**, 4872 (2003); https://doi.org/10.1002/anie.200200565
34. R.J. Morris, R.J. Najmanovich, A. Kahraman and J.M. Thornton, *Bioinformatics*, **21**, 2347 (2005); https://doi.org/10.1093/bioinformatics/bti337
35. A. Kahraman, R.J. Morris, R.A. Laskowski and J.M. Thornton, *J. Mol. Biol.*, **368**, 283 (2007); https://doi.org/10.1016/j.jmb.2007.01.086
36. P.S. Suresh, A. Kumar, R. Kumar and V.P. Singh, *J. Mol. Graph. Model.*, **26**, 845 (2008); https://doi.org/10.1016/j.jmgm.2007.05.005
37. A. Gopalakrishnan, M. Nandhagopal, M. Narayanasamy, C. Sivakumar, M. Vanjinathan and A.S. Nasar, *J. Polym. Sci.*, **62**, 5467 (2024); https://doi.org/10.1002/pol.20240496
38. D. Shivakumar, J. Williams, Y. Wu, W. Damm, J. Shelley and W. Sherman, *J. Chem. Theor. Comput.*, **6**, 1509 (2010); https://doi.org/10.1021/ct900587b
39. H. Rau, *Angew. Chem. Int. Ed. Engl.*, **12**, 224 (1973); https://doi.org/10.1002/anie.197302241
40. G. Rabbani, M.H. Baig, E.J. Lee, W.K. Cho, J.Y. Ma and I. Choi, *Mol. Pharm.*, **14**, 1656 (2017); https://doi.org/10.1021/acs.molpharmaceut.6b01124
41. F. Sun, W. Zong, R. Liu, J. Chai and Y. Liu, *Spectrochim. Acta A Mol. Biomol. Spectrosc.*, **76**, 142 (2010); https://doi.org/10.1016/j.saa.2010.03.002
42. F.-F. Tian, F.-L. Jiang, X.-L. Han, C. Xiang, Y.-S. Ge, J.-H. Li, Y. Zhang, R. Li, X.-L. Ding and Y. Liu, *J. Phys. Chem. B*, **114**, 14842 (2010); https://doi.org/10.1021/jp105766n
43. P.O. Vardevanyan, A.P. Antonyan, M.A. Parsadanyan, M.A. Shahinyan and M.S. Mikaelyan, *Biophys. Rev. Lett.*, **14**, 17 (2019); https://doi.org/10.1142/S1793048019500012
44. Y. Lu, S. Li, H. Xu, T. Zhang, X. Lin and X. Wu, *J. Agric. Food Chem.*, **66**, 9794 (2018); https://doi.org/10.1021/acs.jafc.8b03410
45. A. Sułkowska, *J. Mol. Struct.*, **614**, 227 (2002); https://doi.org/10.1016/S0022-2860(02)00256-9
46. K. Rajendran and R. Peruma, *J. Lumin.*, **130**, 1203 (2010); https://doi.org/10.1016/j.jlumin.2010.02.022
47. R.A. Cox, eds.: L. Grossman and K. Moldave, The Use of Guanidinium Chloride in the Isolation of Nucleic Acids, In: Methods in Enzymology, Academic: New York, vol 12, pp. 120-129 (1968).
48. N. Sarkar, K. Das, D. Nath and K. Bhattacharyya, *Chem. Phys. Lett.*, **196**, 491 (1992); https://doi.org/10.1016/0009-2614(92)85726-Q
49. R. Kumaran and P. Ramamurthy, *J. Fluoresc.*, **21**, 1499 (2011); https://doi.org/10.1007/s10895-011-0836-0
50. E. Ahmad, G. Rabbani, N. Zaidi, S. Singh, M. Rehan, M.M. Khan, S.K. Rahman, Z. Quadri, M. Shadab, M.T. Ashraf, N. Subbarao, R. Bhat and R.H. Khan, *PLoS One*, **6**, e26186 (2011); https://doi.org/10.1371/journal.pone.0026186